

Fabrication of controllable random micro-structured surface by using FTS-based diamond turning

Shigeru Tanikawa, Jiwang Yan*

Department of Mechanical Engineering, Keio University, 3-14-1, Hiyoshi, Kohoku-ku, Yokohama, 223-8522, Japan

*yan@mech.keio.ac.jp

Abstract

Random micro-structured surfaces (RSS) have great application potentials as various functional surface elements, such as optical diffusers and hydrophobic/hydrophilic surfaces. Conventional fabrication methods for RSS, such as chemical etching, are no longer suitable for modern requirements of high precision and controllability. In this study, a novel method was proposed for fabricating controllable random dimple arrays by using fast tool servo (FTS)-based single-point diamond turning. Firstly, small patches of quadratic surfaces were periodically arranged over a large surface area. Then the position, height, and size of each quadratic surface were adjusted by applying random values whose dynamic range is preset. In this way, the spatial difference between the dimples were under control within an adjustable range. Finally, the fabricated surface was evaluated to validate the effectiveness of the proposed method. Results showed that the machined surface feature matched precisely with the designed one. This method provides possibility for mass production of high-precision RSS by patterning mold inserts for molding/imprinting processes.

Keywords: random micro-structured surface, diamond turning, fast tool servo, optical diffuser, freeform surface, dimple array

1. Introduction

Random micro-structured surface (RSS) is commonly used for light diffusion in the optical field. Especially, randomized microlens array makes it possible to achieve homogenized light diffusion while controlling the intensity profile of incident light [1]. Since light diffusion technology has an important application in beam shaping, projectors, 3D sensing, and so forth, several fabrication methods such as dry/wet etching, laser processing, and photolithography [1-3] have been developed. However, these methods cannot control the randomness perfectly, which makes it difficult to predict the machined RSS and fabricate an ideal surface. In this study, a novel method was proposed for fabricating controllable random dimple arrays by using fast tool servo (FTS)-based single-point diamond turning. This method enables flexible control of randomness, and in turn, high-precision machining of an ideal RSS.

2. Designing procedures of RSS

An RSS is composed of dimples with random quadratic surfaces which can be expressed as:

$$z = a(x - b)^2 + c(y - d)^2 + e \quad (1)$$

where x , y , z are variables for each axis, a , b , c , d , and e are shape parameters for controlling the size and position of a dimple along X- and Y-axes, and the depth of the dimple, respectively, as shown in Figure 1. By generating random numbers for the shape parameters, each dimple has a random quadratic surface. In addition, the shape of each dimple is controllable by presetting dynamic ranges of random values. Consequently, an RSS can be created by placing each dimple at a predetermined position. A designed surface formed by these arranged dimples is defined by selecting and combining the smallest overlapping values in the Z-axis direction. Based on the above method, controllable random micro-structured surfaces can be created. Figure 2 demonstrates an RSS generated by the proposed method, which was constituted by 576 (24x24) dimples in total. The diameter and height of basic quadratic surface of dimples were 100 μm

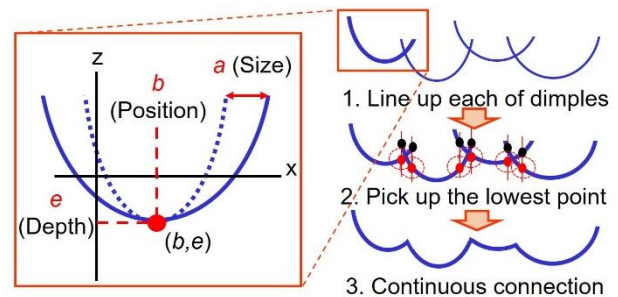


Figure 1. Procedure of RSS design

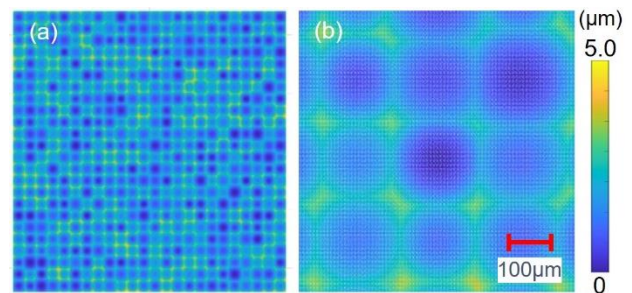


Figure 2. Designed RSS for cutting experiment using developed program: (a) overall, and (b) enlarged view

and 5 μm , respectively. Randomness was applied to each dimple by substituting a random value ranging from 0.45 to 1 for shape parameters a and c , and 0.6 to 1 for e .

3. Experimental setup and procedures

To fabricate the designed RSS, a tool path program with compensation of tool geometry was generated. Then, diamond turning was performed by using a fast tool servo FTS-5000 (AMETEK Precitech Inc.), equipped on an ultraprecision lathe Nanoform X (AMETEK Precitech Inc.). A round-nosed single-

crystal diamond tool with a nose radius of 0.09 mm, a rake angle of 0°, and a clearance angle of 17° was used. The feed rate, depth of cut, and spindle rotation rate were 5 $\mu\text{m}/\text{rev}$, 3.0 μm , and 100 rpm, respectively. Oxygen-free copper with a diameter of 20 mm was used as workpiece. After machining, an optical microscope VHX1000 (KEYENCE Co., Ltd.) and a white-light interferometer Talysurf CCI1000 (AMETEK Co., Ltd.) were used to observe and measure the machined RSS.

4. Results and discussion

4.1. Observation of machined surface

Figure 3(a) shows the measured topography image of a machined RSS, and Figure 3(b) shows the error map created by fitting the measured topography of machined RSS to the designed surface topography in Figure 2(b). From the error map, it can be found that the size, depth and edge position of each quadratic surface in the machined surface matched with those in the design surface. The PV and RMS value of the form error were 425 nm and 52 nm, which indicates that high-precision machining of the designed RSS was achieved in this experiment. This result validates that the randomness of RSS can be controlled by the proposed design method and the fabrication of high-precision RSS can be realized by FTS-based diamond turning. In addition, this method allows predicting the topography of the machined RSS from the design surface, which is difficult to achieve by using conventional fabrication methods.

4.2. Mechanism of edge distortion

Figure 4 shows topography images of the machined RSS at the workpiece center and outer area. Sharp edges were formed between the dimples near the workpiece center, while distorted edges were formed in outer area. Interpolation errors in the toolpath program are considered to be the cause of edge distortion.

As shown in Figure 5, the toolpath program was defined by individual cutting points placed by a constant angle. The equiangular arrangement of the cutting points results in a dense arrangement of cutting points in the center area and a sparse one in the outer area. Between the cutting points, cutting is performed at a tool position determined by interpolation based on neighbouring cutting points. The interpolation error, which is the difference between the designed surface and interpolated curve, depends on the density of cutting points and the complexity of the designed surface. The outer cutting points are sparse, causing a bigger interpolation error which may have distorted the outer edge of the machined RSS.

Simulation was done to predict the machined surface by compensating the interpolation error in the toolpath program. Figure 6 shows a comparison between the predicted edge cross-sectional profiles of the center and outer region of the RSS. The edge cross section in Figure 6 corresponds to the red dashed lines in Figure 4. The measured edge cross section is generally consistent with the predicted one, confirming that the interpolation error in the toolpath program is the main cause of the edge distortion. It is a future work to reduce this error.

5. Conclusions

A program was developed for RSS design, and the designed RSS was successfully machined by diamond turning using an FTS. Unlike conventional methods, the proposed method enables to control the RSS's randomness by changing dynamic range of random values applied to quadratic surfaces. Distortion of dimple edges was produced on the outer area of the machined RSS due to the interpolation error. Suppression of edge distortion will be further investigated in our future work.

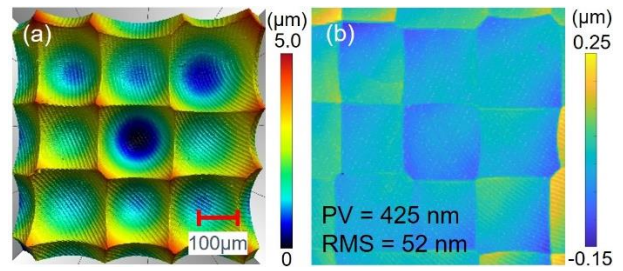


Figure 3. (a) Topography of a machined RSS corresponding to the surface in Figure 2(b); (b) error map created by comparing Figures 2(b) and 3(a).

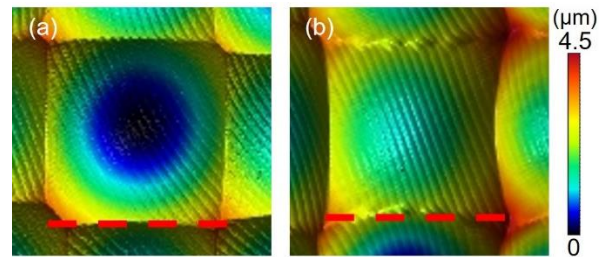


Figure 4. Topography image of (a) a dimple in workpiece center area, and (b) another dimple in the outer area

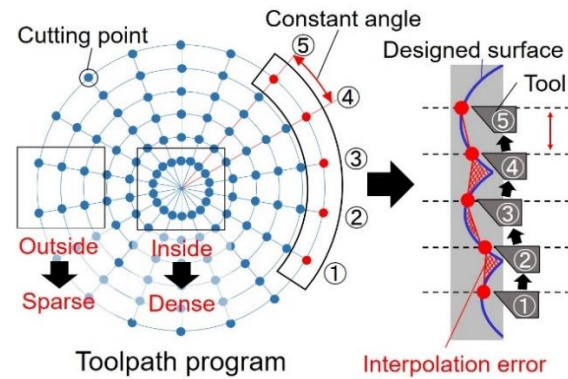


Figure 5. Interpolation error in toolpath program generation

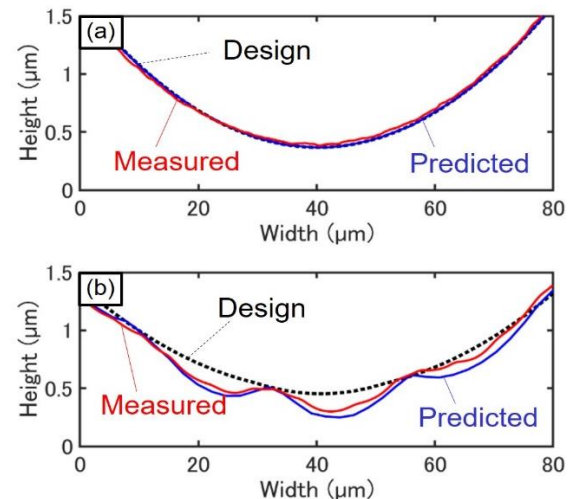


Figure 6. Comparison of simulated and measured edge cross-sectional profiles at (a) workpiece center and (b) outer area

References

- [1] Tasso R. M. Sales 2003 *J. Opt. Eng.* **42** 3084-85
- [2] Meng X, Chen F, Yang Q, Bian H, Du G and Hou X 2015. *J. Appl. Phys. A.* **121** 157-62
- [3] Ruffieux P, Scharf T, Philipoussis, Herzig P H, Voelkel R and Weible J K 2008. *J. Opt. Exp.* **16** 19541-49